

# Imaging artificial caries under composite sealants and restorations

Robert S. Jones  
Michal Staninec  
Daniel Fried

University of California  
Department of Preventive and Restorative  
Dental Sciences  
San Francisco, California 94143-0758  
E-mail: dfried@itsa.ucsf.edu

**Abstract.** Polarization-sensitive optical coherence tomography (PS-OCT) is used to monitor the progression of simulated caries lesions on occlusal surfaces and image the lesions underneath composite sealants. The polarization-sensitive system, recording images in both the parallel and perpendicular axes, is useful for enhancing the image contrast of the artificial caries and minimizing the interference of the strong reflections at surface interfaces. Using the perpendicular-axis signal, the mean reflectivity increase from day 0 to day 14 is 5.1 dB ( $p < 0.01$ , repeated-measures analysis of variation, Tukey-Kramer). For imaging lesions underneath the sealants, the mean reflectivity of the enamel underneath 250, 500, 750, and 1000  $\mu\text{m}$  of composite is calculated for demineralized and control samples. The artificial lesions can be detected under 750  $\mu\text{m}$  of visibly opaque sealant, with a 5.0-dB difference from the control samples (t-test,  $p < 0.001$ ). Tooth colored sealants allow deeper imaging depth. The artificial lesions could be detected under 1000  $\mu\text{m}$  of sealant, with a 6.6-dB difference from the control samples (t-test,  $p < 0.001$ ). This study demonstrates that PS-OCT can be used to track lesion progression on occlusal surfaces nondestructively with or without sealants. © 2004 Society of Photo-Optical Instrumentation Engineers. [DOI: 10.1117/1.1805562]

Keywords: polarization-sensitive optical coherence tomography; dental caries; composite sealants.

Paper 04029 received Mar. 2, 2004; revised manuscript received May 5, 2004; accepted for publication May 7, 2004.

## 1 Introduction

The occlusal pits and fissures of posterior teeth continue to be the principal area where dental decay (caries) develops. Occlusal caries are difficult to detect and monitor, particularly in the early stages, using the conventional armamentarium of the dental explorer and bitewing x-rays. Since pit and fissures are highly susceptible to caries, clinicians often place preventive resin sealants on the occlusal surfaces of posterior teeth on patients with deep fissures or a history of caries. Although resin sealants prevent decay by acting as a physical barrier blocking out acid-producing bacteria, the adhesion of the sealant to the tooth enamel can eventually fail and dental caries can develop underneath the sealant restorations.<sup>1</sup> No current diagnostic method is capable of evaluating the structural integrity of resin sealants and detecting caries under these materials.

Polarization-sensitive optical coherence tomography (PS-OCT) is a noninvasive technique for creating cross sectional images of internal biological structures.<sup>2,3</sup> Utilizing low-coherence interferometry, OCT is capable of measuring backscattered light as a function of optical depth in up to 2 to 3 mm of dental enamel with  $\sim 10$  to 30  $\mu\text{m}$  of resolution.<sup>4–6</sup> Enamel is the outer layer of a tooth (the first tissue usually infected by dental decay), and is birefringent due to the rod-

like organization of the hydroxyapatite crystals.<sup>7</sup> PS-OCT systems can operate with near-IR light, especially near 1310 nm, which significantly improves the axial imaging penetration depth over wavelengths in the visible range, since dental enamel has been shown to be nearly transparent in the near-IR.<sup>8–10</sup> Carious enamel highly scatters near-IR light, and OCT can measure this increased backscattered intensity.<sup>5,11,12</sup> Initial PS-OCT images by Baumgartner et al.<sup>11</sup> resolved enamel demineralization through an increase in backscattered intensity and changes in the enamel birefringence. Later studies demonstrated that if the incident illuminating light is polarized, the carious tissue will also rapidly depolarize the light.<sup>5</sup> PS-OCT can be used to determine the degree of depolarization of the backscattered light. The strong reflection at the tooth surface can be a confounding factor in detecting caries by masking the light reflected from a demineralized lesion. Polarized light can be exploited to minimize the effects of this reflected light and enhance the image contrast of carious lesions.

PS-OCT has been used to image the artificial caries progression on facial enamel surfaces by measuring the high backscattered reflectivity and depolarization of carious lesions.<sup>13</sup> The PS-OCT system operating at 1310 nm utilized linearly polarized incident light and recorded images in axes parallel or perpendicular to the incident light. This previous study by our group correlated the degree of depolarization with the severity of the demineralization of the caries lesions. Lesion severity was quantified by measuring the intensity of the linearly polarized light scattered (depolarized) into the

Address all correspondence to: Daniel Fried, Univ. of California/San Francisco, Dept. of Preventive & Restorative Dental Sciences, 707 Parnassus Ave., San Francisco, CA 94143-0758. Tel: 415-502-6641; Fax: 415-502-6642; E-mail: dfried@itsa.ucsf.edu

perpendicular axis. These studies illustrated that PS-OCT can be used to image early enamel smooth surface caries. Most new caries lesions, however, are not found on smooth surfaces, but rather involve diagnostically challenging regions like the occlusal surfaces.<sup>14</sup> Therefore, the method used to quantify lesion severity must be insensitive to the surface topography of the tooth. Recent investigations of dental composite materials, Otis et al., have used OCT to discriminate composite sealants from sound enamel tissue.<sup>15</sup> In addition, Feldchtein et al. observed that PS-OCT cannot only identify composites, but image dentinal caries beneath these materials.<sup>16</sup> However, a method to quantify the severity of decay in occlusal surfaces and beneath composite sealants and restorations has not been demonstrated. The objective of this study was to use an all-fiber-based PS-OCT system operating at 1310 nm to image and quantify artificial caries progression on the occlusal surfaces of posterior teeth and artificial occlusal caries underneath resin sealants.

## 2 Materials and Methods

### 2.1 Artificial Occlusal Caries

45 sound human posterior teeth were mounted on 12×12-mm acrylic blocks after root resection. Teeth were sterilized using gamma irradiation and stored in a moist environment to preserve tissue hydration with 0.1% thymol added to prevent bacterial growth. Teeth were not chemically or mechanically pretreated before the study. An acid resistant varnish was applied on the teeth on all areas outside the 4×3-mm pit and fissure region, which was scanned using the PS-OCT system. Artificial occlusal lesions on 20 teeth were formed using a well-characterized pH cycling model replicating the cycle of demineralization and remineralization that takes place naturally in the oral environment.<sup>17,18</sup> Teeth were exposed for 14 days to a daily regimen of 6-h demineralization and 17-h remineralization.<sup>19</sup> Teeth were exposed 6 h each day to a demineralizing solution of 40-mL aliquots of a buffer solution containing 2.0-mmol/L calcium, 2.0-mmol/L phosphate and 0.075-mol/L acetate maintained at pH 4.3 and a temperature of 37 °C. After demineralization, teeth were immersed for 17 h in a 20-mL remineralization solution of 1.5-mmol/L calcium, 0.9-mmol/L phosphate, 150-mmol/L KCl, 20-mmol/L cacodylate buffer maintained at pH 7.0 and 37 °C. Five teeth were imaged periodically at day 0, 1, 3, 6, 9, and 14 during the pH cycling regimen. 20 teeth were used as nontreated controls.

### 2.2 Sealant Restorations

After artificial caries were created on the occlusal surfaces, approximately 1-mm-thick layer of resin sealant was placed over the pits and fissures of the 20 teeth. Two sealant materials, Aeliteflo™ (Bisco) ( $n=10$ ) and Concise™ (3M ESPE) ( $n=10$ ), were used in this study. Both sealants are primarily composed of a matrix resin methacrylate monomer. Concise™ is a visibly opaque sealant and has 5 to 10% by weight of silica filler,<sup>20</sup> which provides strength and resistance to long-term wear. A tooth colored dental shade (A3) was selected for the Aeliteflo™ sealant (40 to 70% filler).<sup>21</sup> For the 20 control teeth, teeth were etched with 35% phosphoric acid for 15 s, rinsed with water, and dried before sealant application. This acid etching is required for adequate bonding of the

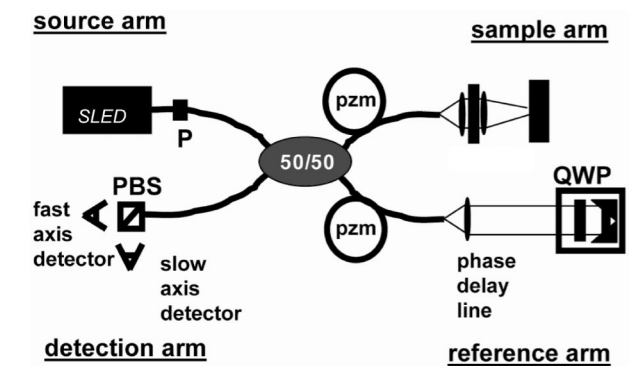


**Fig. 1** PS-OCT system—light from the SLED is linearly polarized and coupled into the slow axis of polarization maintaining fiber and equally split between the sample and reference arms of a fiber optic Michelson interferometer. The path length difference between the sample and reference arms are varied using piezoelectric fiber stretchers (pzm). The maximum path length difference varied by 5.74 mm at a rate of 150 Hz. A polarizing beamsplitter (PBS) in the detection arm splits the fast (perpendicular) and slow (parallel) axis components of the light onto the two detectors.

sealant material to the dental enamel. In addition to sealants, composite materials used in restorative cavity preparations were also studied by fabricating 1.25-mm-thick blocks of Z-100™ (A3, 3M ESPE) and Herculite™ (A2, Kerr) composites. The composite materials, along with blocks of Aeliteflo™ and Concise™, were placed over an intense scattering surface of barium sulfate.

### 2.3 Polarization Sensitive Optical Coherence Tomographic Imaging

An all-fiber-based optical coherence domain reflectometer (OCDR) with polarization maintaining (PM) optical fiber, high-speed piezoelectric fiber stretchers, and two balanced InGaAs detectors that were custom designed and fabricated by Optiphase, Incorporated (Van Nuys, California) was used to acquire the images presented. This two-channel system was coupled with a 3.5-mW power superluminescent diode (SLD) source, centered at 1310 nm, and possessed a spectral bandwidth full width at half maximum (FWHM) of 25 nm. This diode source was used for the samples that were monitored throughout the pH cycling regimen. For samples in the sealant experiment, the OCDR system was coupled with a superluminescent diode (SLD), SLED-1310, from COVEGA (Jessup, Maryland), with an output power of 20 mW, a center wavelength of 1310 nm, and a spectral bandwidth (FWHM) of 50 nm. A high speed xy-scanning system with an ESP 300 controller and 850G-HS stages from Newport Corporation (Irving, California) was integrated with the system for *in vitro* optical tomography. A schematic of the system based on a polarization-sensitive Michelson white light interferometer is shown in Fig. 1 and was described previously.<sup>13</sup> Light from each SLD was linearly polarized and coupled into the slow axis of the polarization maintaining fiber and passed through a linear polarizer. The incident beam was focused onto the sample surface using a 20-mm focal length antireflective-coated plano-convex lens. This configuration provided lateral resolution of 30  $\mu\text{m}$  and an axial resolution of 20  $\mu\text{m}$ . The system was found to have a signal-to-noise ratio (SNR) of 40

dB, which was calculated using a single reflective signal that was just below that saturation intensity of the InGaAs detectors.

Linearly polarized light illuminated the tooth samples, and the reflected/backscattered intensity in both orthogonal polarizations was coupled into the slow (parallel) and fast (perpendicular) axes of the PM fiber of the sample arm (Fig. 1). The signal intensity for each polarization state, defined as the parallel and perpendicular axes, was measured from each detector channel after the signals were electronically demodulated. The PS-OCT system was completely controlled using Labview™ software from National Instruments (Austin, Texas). Two-dimensional OCT intensity plots were obtained by collecting a series of depth-resolved signals by laterally scanning the beam across the tooth. The acrylic blocks attached to each tooth fit into a custom metal jig that allowed orientation and coordinates to be precisely replicated, within 50  $\mu\text{m}$ , for every scan.<sup>22</sup>

Transverse *b*-scan images from both polarization states were acquired at day 0, 1, 3, 6, 9, and 14 during the 14-day pH cycling regimen for five teeth. In the perpendicular-axis images, the mean reflectivity of the enamel was determined by integrating the enamel 200  $\mu\text{m}$  deep and dividing by the total pixels integrated. After day 14 of the PS-OCT scans, teeth were sectioned and examined under a polarized light microscope (100 $\times$ ) to compare the artificial lesion depth with the OCT perpendicular-axis images. For the other 40 sample teeth, images were acquired at day 0, and for the treatment samples, also after 14 days of pH cycling. Following the PS-OCT scans of the artificial lesions ( $n=20$ ) and control samples ( $n=20$ ), the Aeliteflo™ and Concise™ sealants were applied to the occlusal surfaces of the posterior teeth. To determine how deep the lesions could be detected under the sealants, the mean reflectivity of the demineralized samples and the controls was calculated under different optical depths of sealant: 250, 500, 750, and 1000  $\mu\text{m}$ . PS-OCT was also used to image an intense scattering surface of barium sulfate through 1.25-mm-thick blocks of Concise™, Aeliteflo™, Herculite™, and Z-100™. Image analysis was performed using Matlab™ (Mathworks, Natick, Massachusetts) and Igor Pro™ (Wavemetrics Incorporated, Lake Oswego, Oregon).

### 3 Results

#### 3.1 Imaging Artificial Caries Progression on Occlusal Surfaces

Initial, day 0, images of an occlusal surface illuminated with the 3.5-mW source are shown in Fig. 2(a). Incident light on a sample is linearly polarized, and the backscattered light was recorded in both the parallel and perpendicular axes to the original incidence. The parallel- and perpendicular-axis images are presented in a logarithmic grayscale, recorded in decibels (dB), where white represents high backscattering or reflection. Images of the dental enamel at day 0 constructed from the parallel axis show an intense surface reflection at the enamel-air interface and 1 mm of depth penetration. Figure 2(a) shows the progression of the lesion severity in depth and reflectivity in the perpendicular-axis images. The parallel-axis image at day 14 [Fig. 2(a)] reveals the higher reflectivity or scattering from the subsurface lesion, but compared with perpendicular-axis images, does not provide as high a contrast

with day 0. The mean reflectivity was calculated for each time point in the perpendicular-axis images for all five samples illuminated with the 3.5-mW source. In the pH cycling model, the depth and severity of the lesion increases as the square root of the time,<sup>13,23</sup> therefore, the mean reflectivity  $\pm$ s.d. was plotted versus the square root of pH cycling time [Fig. 2(b)]. There was a linear increase in the mean reflectivity with the square root of time,  $r=0.94$ . This strong correlation indicates that the perpendicular-axis images represent the progressing severity of the artificial lesions. The mean reflectivity of the lesion became significant compared with day 0 after day 9 [ $p<0.05$ , repeated-measures analysis of variation (ANOVA); Tukey-Kramer]. The mean reflectivity increase from day 0 to day 14 was 5.1 dB ( $p<0.01$ ), which is equivalent to a three-times-larger reflectivity intensity, since decibels are log scale units of optical power. After sectioning the teeth, the samples under polarized light revealed that the real depth of the pH cycled artificial lesions were  $\sim 100 \mu\text{m}$ , which validated that the 200- $\mu\text{m}$  optical depth integrations transverse the entire artificial lesions ( $n=1.60$ ).

#### 3.2 Imaging Artificial Caries Underneath Dental Sealants

PS-OCT *b*-scan images of the control samples with no occlusal decay are shown in Fig. 3(a). Concise™ sealant is placed over the occlusal surface, and from the parallel-axis image it is evident that the Concise™ sealant strongly backscatters the incident light. The backscattered light is also depolarized, which is illustrated by the high reflectivity of the sealant in the perpendicular-axis image. For the pH cycled samples, images of the artificial lesions on the occlusal surfaces were acquired [Fig. 4(a)]. After Concise™ sealant was placed over the occlusal surfaces, the PS-OCT *b*-scans were able to image the artificial lesions beneath the margin of the sealant but at a limited depth. Analyzing the perpendicular-axis images, the mean reflectivity of the enamel underneath 250, 500, 750, and 1000  $\mu\text{m}$  of Concise™ sealant was calculated for the treatment and control samples [Fig. 5(a)]. The artificial lesions could be detected under 750  $\mu\text{m}$  of the Concise™ sealant, with a 5.0-dB difference from the control samples (t-test,  $p<0.001$ ).

When examining the Aeliteflo™ samples, the PS-OCT *b*-scans of the control samples show an imaging penetration depth that was markedly greater than the Concise™ sealant [Fig. 3(b)]. This can be attributed to the weaker backscattering seen in the parallel-axis image. As indicated in the perpendicular-axis image, the Aeliteflo™ sealant does not significantly depolarize the incident light. For the pH cycled and control samples, the mean reflectivity of the enamel in the perpendicular-axis images was calculated underneath 250, 500, 750, and 1000  $\mu\text{m}$  of Aeliteflo™ sealant [Fig. 5(b)]. The artificial lesions could be detected under the entire 1 mm of the Aeliteflo™ sealant [Fig. 4(b)], with a 6.6-dB difference from the control samples (t-test,  $p<0.001$ ). To examine the potential of imaging through composite restorative materials, PS-OCT *b*-scans were acquired through 1.25-mm-thick sections of Concise™, Aeliteflo™ (A2, Bisco), Herculite™ (A2, Kerr), and Z-100™ (A3,3M) with an intense scattering surface underneath the materials. The scattering surface was resolved in both the parallel- and perpendicular-axes images

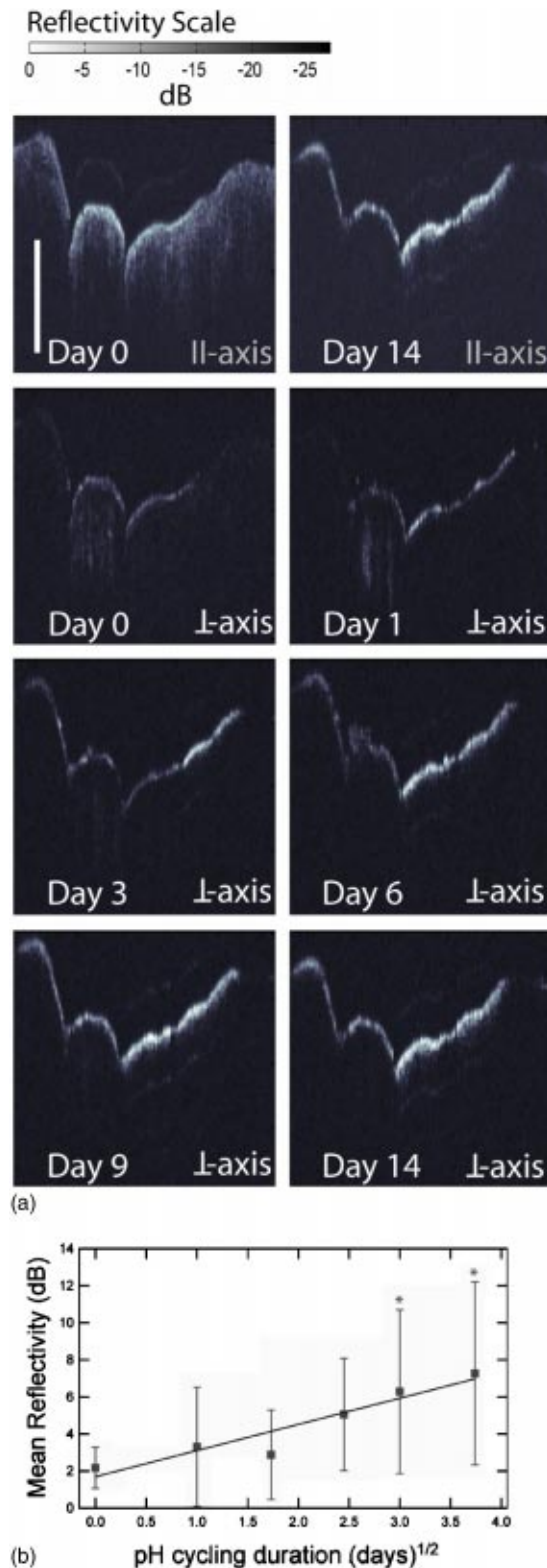


**Fig. 2** (a) PS-OCT images, illuminated with the 3.5-mW SLD, are viewed using a logarithmic grayscale measured in decibels. (a) The reflectivity increase from day 0 to day 14 is difficult to quantify using the parallel-axis images due to the high surface reflection. Perpendicular-axis images at day 0, 1, 3, 6, 9, and 14 recorded the growing severity of the artificial lesions in both depth and reflectivity. The secondary coherence artifact, or “ghost image” above the occlusal surface, is caused by internal reflections within the optical fiber of the sample probe. The white bar is 1 mm of optical depth. (b) The mean reflectivity (error bars=standard deviation) was plotted versus the square root of time. With the 3.5-mW 25-nm bandwidth SLD source, the mean reflectivity versus the square root of time showed a linear relationship,  $r=0.94$  ( $n=5$ ).

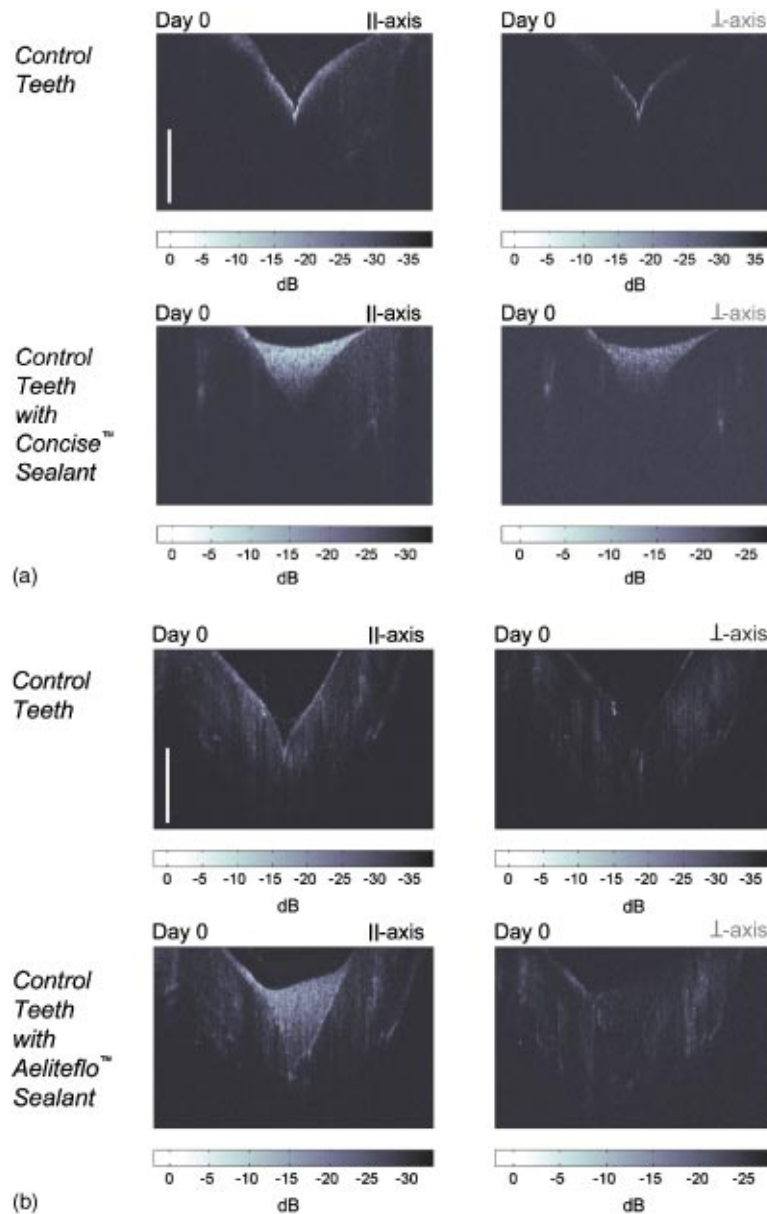


**Fig. 3** (a) PS-OCT images of the control teeth, at day 0, were recorded in the parallel and perpendicular axes and were illuminated with the 20-mW SLD. The images through Concise<sup>™</sup> show that the material highly reflects and depolarizes the incident light. Imaging penetration depth is limited. (b) Images through Aeliteflo<sup>™</sup> show markedly higher imaging penetration depth and less reflectivity and depolarization. The white bar is 1 mm of optical depth.

through all of the materials except the Concise<sup>™</sup> sealant (Fig. 6).

#### 4 Conclusion

This study demonstrates that PS-OCT can effectively monitor and quantify the artificial lesion progression on occlusal surfaces and image demineralized enamel under resin sealants. Initial studies have primarily studied the ability of OCT to image demineralization on bovine<sup>24</sup> or human smooth surface enamel samples.<sup>13</sup> Although an important step in OCT development in dentistry, diagnosing smooth surface decay does not pose the same clinical challenges as detecting occlusal surface caries. Caries on the occlusal surfaces are also more prevalent in children and adults than on smooth surfaces. In

addition, caries under dental sealants are a serious and widespread problem in dentistry, and this study demonstrates for the first time that decay under sealants can be quantified with OCT. This study further indicates the clinical utility of OCT, especially a polarization-sensitive system.

By using linearly polarized incident light, PS-OCT can detect subsurface lesions by an increase in both backscattering and depolarization. Without a polarization-sensitive system, the strong surface reflection, which also causes secondary coherence peaks, can both obscure and resemble the signal of subsurface demineralization of the lesion, as illustrated in the boxed areas of Fig. 4(a). The signal in the perpendicular axis is not sensitive to this surface reflection, because incident light is not depolarized on surface reflection at normal inci-

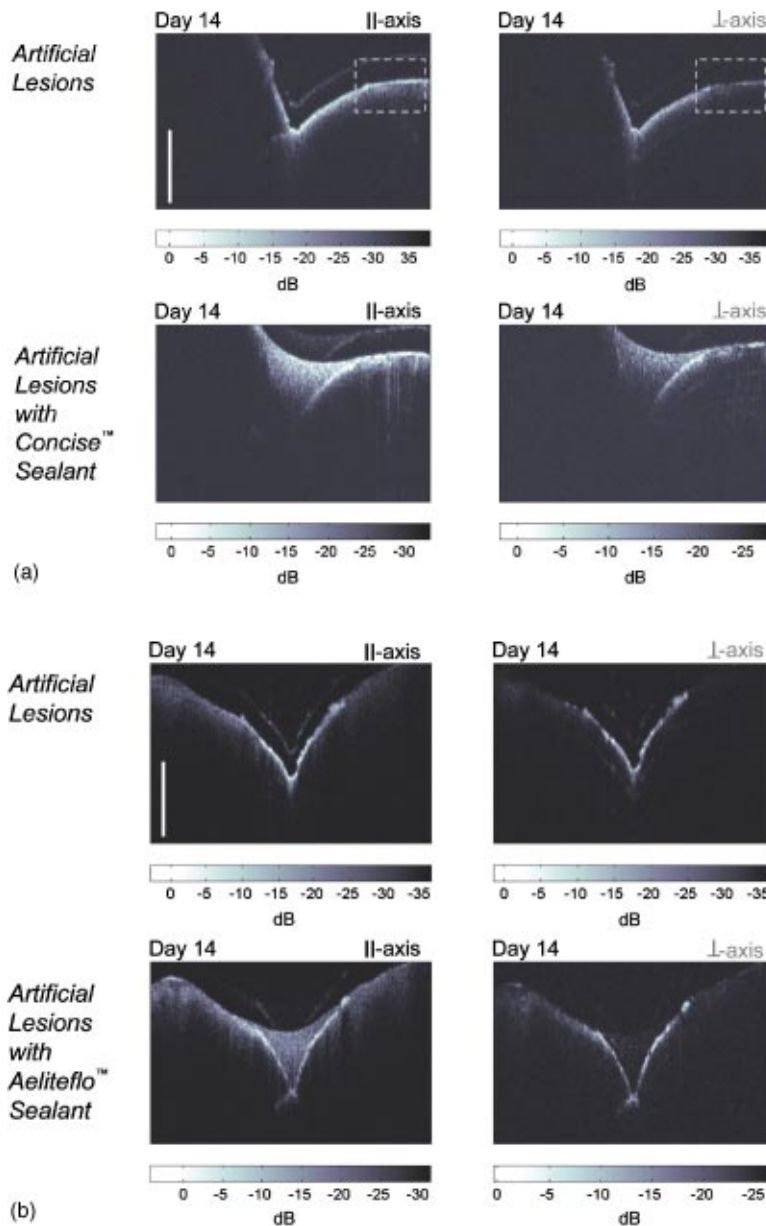


**Fig. 4** (a) PS-OCT images of teeth that have artificial occlusal lesions from 14-day pH cycling. In the parallel axis, surface reflections (box) can mask the subsurface demineralization. The perpendicular axis records depolarization and the acid exposed lesion area is easily differentiated from the occlusal surface that was protected from demineralization. PS-OCT is able to detect the artificial lesion beneath the margin of the Concise™ sealant but at a limited depth. (b) The artificial lesions can be imaged through the full depth of the Aeliteflo™ sealant samples. The white bar is 1 mm of optical depth.

ence. In sound enamel, the images constructed from the perpendicular axis are expected to be less intense than the parallel axis, since the perpendicular-axis signal intensity arises from the polarization rotation of the incident light by the enamel birefringence. As a caries lesion develops, the subsurface demineralized areas strongly scatter the incident light, contributing to a higher reflectivity signal in both axes. The strong scattering also causes rapid depolarization, which increases the signal in the perpendicular axis to a greater degree than that caused by the sound enamel birefringence. Birefringence is particularly problematic in conventional OCT systems because it produces artifacts, such as banding, that confounds early caries diagnosis.<sup>4</sup>

We demonstrate that occlusal lesion severity can be quantified by measuring the increased signal intensity of light depolarized into the perpendicular axis. The enamel signal in the perpendicular-axis images can be directly integrated to determine the overall lesion severity. Other studies have reported that demineralization can be detected in a conventional OCT system by measuring the attenuation of the signal or reflectivity loss compared with the surrounding healthy tissue.<sup>24</sup> This approach assumes that imaging depths are similar throughout a *b*-scan. Imaging penetration and attenuation of a signal can be influenced by the varying angle of incidence seen when scanning occlusal surfaces. Polarization-sensitive OCT *b*-scans, which are presented in total intensity and de-

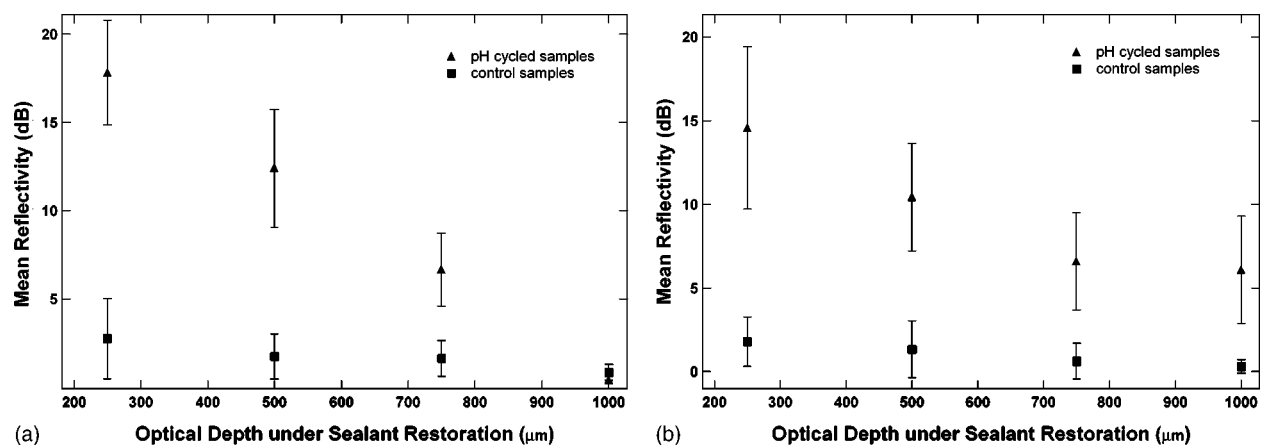


**Fig. 5** The mean reflectivity of the artificial lesions and the controls under different optical depths of the sealants were calculated using the perpendicular-axis image. In the perpendicular-axis, the total reflectivity was integrated  $\sim 100 \mu\text{m}$  deep in the enamel and divided by the total pixels integrated. This mean reflectivity was calculated under different depths of the sealant. (a) For the Concise™ samples, the lesions could be imaged up to  $750 \mu\text{m}$  deep with 5.0-dB difference from the control samples (t-test,  $p < 0.001$ ). (b) For the Aeliteflo™ samples, the artificial lesions could be detected under the full 1 mm depth of the sealant we placed, with a 6.6-dB difference from the control samples (t-test,  $p < 0.001$ ).

gree of polarization images, have shown improved contrast in detecting caries lesions than using only reflectivity.<sup>11</sup> In healthy enamel, the degree of polarization, if measured as a difference between the two orthogonal axes divided by the total intensity, will alternate between  $-1$  and  $1$  as the polarized light travels through the tissue. The birefringence of dental enamel is lost as it undergoes demineralization, and therefore the degree of depolarization will be close to zero after it passes through the demineralization. Measuring the degree of depolarization gives better contrast between healthy and carious enamel than total intensity, but this method is also sensitive to the orientation of the incident light to the optical axis of the tissue. The PS-OCT system presented is affected by

enamel birefringence that causes incident light to rotate into the perpendicular axis. However, the contribution from the strong scattering of enamel demineralization in the perpendicular-axis signal is orders of magnitude greater than that caused by polarization rotation.

For the sealant samples, PS-OCT imaged the artificial caries in both polarization axes. This demonstrates that conventional OCT could detect the lesions by an increase in reflectivity, but it is important to note that the image would be sensitive to the marginal adaptation of the sealant to the underlying enamel. Defects in the contact of the sealant to the enamel would produce surface/air interfaces that could highly reflect the incident light. These reflections could only be discriminated with demineralization in a polarization-sensitive system. PS-OCT can quantify the severity of a carious lesion under sealant restorations by directly integrating the backscattered perpendicular-axis signal in the enamel. Sealant and composite materials that do not depolarize the incident light increase the diagnostic ability of PS-OCT to quantify the lesion severity. For the control samples, the surface acid etching needed for bonding did not produce noticeable backscattering signals, which indicates that the artificial lesions were not imaged only by surface scattering events. Intimate adaptation of the sealant to the etched enamel controls may have reduced the surface scattering and depolarization.

The lower imaging depth through Concise™ compared to Aeliteflo™ suggests that the visible light opacifier, titanium dioxide, which is found in Concise™, strongly attenuates even near-IR light.<sup>20</sup> Concise™ is produced in an opaque white shade because the conventional method for detecting caries underneath sealants is visible and tactile inspection. The opaque sealant is preferred by many clinicians, since the margin can be easily differentiated from the enamel. The proprietary oxides that alter the Aeliteflo™ hue do not adversely affect imaging depth, nor does the increase in filler content of Herculite™ and Z-100™. Undoubtedly, a future shift in diagnostic techniques will be accompanied with a change in material composition. Since Aeliteflo™, Herculite™, and Z-100™ are all used for larger cavity restorations in dentistry,

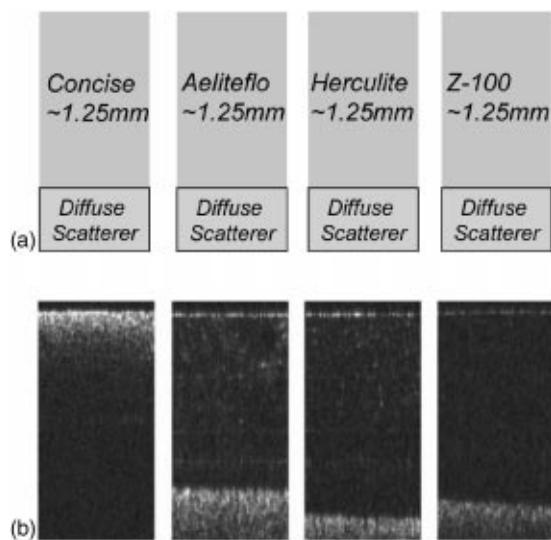


**Fig. 6** (a) Approximately 1.25-mm-thick blocks of Concise™, Aeliteflo™, Herculite™, and Z-100™ were fabricated and an intense diffuse scattering surface of barium sulfate was placed underneath the composites. (b) PS-OCT images through each of the materials are shown in the perpendicular axis. The barium sulfate is revealed in all of the materials except the Concise™ sealant material.

this study illustrates the potential of PS-OCT to image and quantify enamel demineralization under sealant and composite restorations.

### Acknowledgments

This work was supported by NIH/NIDCR grants 1-R01 DE14698 and T32 DE07306-07. The authors would also like to acknowledge the contributions of John D. B. Featherstone, Charles Q. Le, and Larry G. Watanabe.

### References

1. E. A. Kidd and D. Beighton, "Prediction of secondary caries around tooth-colored restorations: a clinical and microbiological study," *J. Dent. Res.* **75**, 1942–1946 (1996).
2. J. A. Izatt, M. R. Hee, D. Huang, J. G. Fujimoto, E. A. Swanson, C. P. Lin, J. S. Schuman, and C. A. Puliafito, in *Medical Optical Tomography: Functional Imaging and Monitoring*, Vol. IS11, G. Muller, B. Chance, R. Alfano, S. Arridge, J. Beuthan, E. Gratton, M. Kaschke, B. Masters, S. Svanberg, and P. v. d. Zee, Eds., pp. 450–472, SPIE Press, Bellingham, WA (1993).
3. J. F. deBoer, T. E. Milner, M. J. C. vanGemert, and J. S. Nelson, "Two-dimensional birefringence imaging in biological tissue by polarization-sensitive optical coherence tomography," *Opt. Lett.* **22**, 934–936 (1997).
4. B. W. Colston, U. S. Sathyam, L. B. DaSilva, M. J. Everett, and P. Stroeve, "Dental OCT," *Opt. Express* **3**, 230–238 (1998).
5. M. J. Everett, B. W. Colston, U. S. Sathyam, L. B. D. Silva, D. Fried, and J. D. B. Featherstone, "Noninvasive diagnosis of early caries with polarization sensitive optical coherence tomography (PS-OCT)," *Proc. SPIE* **3593**, 177–183 (1999).
6. B. T. Amaechi, S. M. Higham, A. G. Podoleanu, J. A. Rogers, and D. A. Jackson, "Use of optical coherence tomography for assessment of dental caries: quantitative procedure," *J. Oral Rehabil.* **28**, 1092–1093 (2001).
7. X. J. Wang, T. E. Milner, J. F. de Boer, Y. Zhang, D. H. Pashley, and J. S. Nelson, "Characterization of dentin and enamel by use of optical coherence tomography," *Appl. Opt.* **38**, 2092–2096 (1999).
8. R. Jones and D. Fried, "Attenuation of 1310-nm and 1550-nm laser light through sound dental enamel," *Proc. SPIE* **4610**, 187–190 (2002).
9. D. Fried, J. D. B. Featherstone, R. E. Glana, and W. Seka, "The nature of light scattering in dental enamel and dentin at visible and near-IR wavelengths," *Appl. Opt.* **34**, 1278–1285 (1995).
10. R. S. Jones, G. D. Huynh, G. C. Jones, and D. Fried, "Near-infrared transillumination at 1310-nm for the imaging of early dental decay," *Opt. Express* **11**, 2259–2265 (2003).
11. A. Baumgartner, C. K. Hitznerberger, S. Dicht, H. Sattmann, A. Moritz, W. Sperr, and A. F. Fercher, "Optical coherence tomography for dental structures," *Proc. SPIE* **3248**, 130–136 (1998).
12. D. Fried, J. Xie, S. Shafi, J. Featherstone, T. M. Breunig, and C. Q. Le, "Imaging caries lesions and lesion progression with polarization optical coherence tomography," *Proc. SPIE* **4610**, 113–124 (2002).
13. D. Fried, J. Xie, S. Shafi, J. D. B. Featherstone, T. Breunig, and C. Q. Lee, "Early detection of dental caries and lesion progression with polarization sensitive optical coherence tomography," *J. Biomed. Opt.* **7**, 618–627 (2002).
14. N. Harris and F. Garcia-Godoy, *Primary Preventive Dentistry*, 5th ed., Appleton & Lange, Stamford, CT (1999).
15. L. L. Otis, R. I. al-Sadhan, J. Meiers, and D. Redford-Badwal, "Identification of occlusal sealants using optical coherence tomography," *J. Clin. Dent.* **14**, 7–10 (2003).
16. F. I. Feldchtein, G. V. Gelikonov, V. M. Gelikonov, R. R. Iksanov, R. V. Kuranov, A. M. Sergeev, N. D. Gladkova, M. N. Ourutina, J. A. Warren, and D. H. Reitze, "In vivo OCT imaging of hard and soft tissue of the oral cavity," *Opt. Express* **3**, 239–251 (1998).
17. D. J. White and J. D. B. Featherstone, "A longitudinal microhardness analysis of fluoride dentifrice effects on lesion progression in vitro," *Caries Res.* **21**, 502–512 (1987).
18. J. D. B. Featherstone, M. M. O'Reilly, M. Shariati, and S. Brugler, in *Factors Relating to Demineralization and Remineralization of the Teeth*, S. A. Leach, Ed., IRL Press, Oxford, UK (1986).
19. J. D. B. Featherstone, R. Glana, M. Shariati, and C. P. Shields, "Dependence of in vitro demineralization and remineralization of dental enamel on fluoride concentration," *J. Dent. Res.* **69**, 620–625 (1990).
20. 3M Material Safety Data Sheet 3M™ ESPE™ Concise™ White Sealant, 3M, St. Paul, MN (2003).
21. Aeliteflo/Aeliteflo LV Material Safety Data Sheet, Bisco, Inc., Schaumburg, IL (2003).
22. R. S. Jones, M. Staninec, and D. Fried, "Imaging secondary caries under composite sealants and restorations," *Proc. SPIE* **5313**, 7–16 (2004).
23. J. D. B. Featherstone, J. M. ten Cate, M. Shariati, and J. Arends, "Comparison of artificial caries-like lesions by quantitative microradiography and microhardness profiles," *Caries Res.* **17**, 385–391 (1983).
24. B. T. Amaechi, A. Podoleanu, S. M. Higham, and D. A. Jackson, "Correlation of quantitative light-induced fluorescence and optical coherence tomography applied for detection and quantification of early dental caries," *J. Biomed. Opt.* **8**, 642–647 (2003).